Throughput Comparison of CDM and TDM for Downlink Packet Transmission in CDMA Systems With a Limited Data Rate Set

Jaeweon Cho, *Member, IEEE,* and Daehyoung Hong, *Member, IEEE*

***Abstract*—Throughputs with code-division multiplexing (CDM) and time-division multiplexing (TDM) for downlink packet transmission are compared in multirate code-division multiple access (CDMA) systems. The authors propose and use a model that can show the impact of self-interference on the received bit energy per noise and interference power density (E_b/N_t). The developed analytical method reflects the effect of a limited data rate set, shadowed radio paths, and a limited number of spreading codes. Performance measures include asymptotic throughput, outage probability, probability of the data rate being limited by the given rate set, and probability of the system throughput being limited by the available number of spreading codes. The system throughput of packet channels for delay-tolerant service is evaluated in a 3GPP WCDMA system model. The authors show that the throughput with CDM can be equal to that with TDM in a fully loaded system without the data rate limitation. It is also shown that CDM can outperform TDM with respect to the asymptotic throughput when one takes into account the self-interference, the limitation on the data rate set, and resource reallocation of users in outage.**

***Index Terms*—Code-division multiple access (CDMA), code-division multiplexing (CDM), code shortage, downlink, multirate transmission, self-interference, throughput, time-division multiplexing (TDM).**

I. Introduction

As THE wireless Internet services have been regarded as one of the major services in the upcoming third and future generation wireless systems, efficient utilization of radio resources on downlink is becoming more important. In multirate code-division multiple access (CDMA) packet systems, radio resources can be assigned in a code or time-division manner [1]. In the code-division approach, a large number of users can have low data rate channels available simultaneously. On the other hand, in the time-division approach, the whole capacity is given to one user or a few users at each moment of time. A combined approach of the two can also be applied. As a base station (BS) transmits to more users simultaneously by code-division multiplexing (CDM), the allocated data rate to a user is decreased but the length of the allocation per user may be increased.

The primary objective of radio resource management policy is to maximize system throughput. In order to achieve it on the CDMA downlink, the multiplexing scheme should be properly applied. The allowable data rate in practical systems is discontinuous and limited to a peak rate. Only a limited number of data rates are used for the user traffic channel.[1] If BS transmits to too few users at a time, in other words, if the number of CDM users is set to be too small, the data rate assigned to a user can be determined by the peak data rate limitation rather than the interference power. On the contrary, if the number of CDM users is set to be too large, the assigned power per user will be so low that even the minimum data rate is not assigned to the user at a poor carrier to interference ratio (C/I) region, i.e., an outage event occurs. Hence, the number of CDM users should be carefully selected so as to maximize the system throughput and also to prevent the outage event.

For the exact evaluation of throughput on the CDMA downlinks, the effects of self-interference as well as multi-user interference must be considered. Multirate services with high data rate can be implemented by variable spreading factor (VSF) or multicode (MC) schemes [2]. Despite employing orthogonal spreading codes on the downlinks, a lack of orthogonality in the multipath fading channels can produce multi-user interference in the same cell. Self-interference within the packet channel of a user is also generated due to small spreading factor (SF) or many MC channels used for high rate transmission [3]. Therefore, as a BS transmits to fewer users at a time, the multi-user interference is decreased but the self-interference is increased, and vice versa.

Previous studies on the downlink throughput did not carefully consider the self-interference and the limited data rate set. System throughput on the uplink can be maximized by allowing only one data user to transmit because the multi-user interference can be avoided by doing so [4]. Bedekar *et al.* [5] applied the same concept to the downlink, and then they showed that it is optimal for BS to transmit to, at most, one data user at a time. Their results were, however, based on the assumption that the self-interference is negligible. Unlike the asynchronous uplink, the self-interference on the synchronous downlink is not much less than the multi-user interference, as shown in the link

Manuscript received May 9, 2002; revised January 18, 2003; accepted February 18, 2003. The editor coordinating the review of this paper and approving it for publication is R. Murch. This work was supported in part by the Basic Research Program of the Korea Science and Engineering Foundation (KOSEF) under grant R01-1999-000-00205-0 and by the Electronics and Telecommunications Research Institute (ETRI).

J. Cho was with the Department of Electronic Engineering, Sogang University, Seoul 121-742, Korea. He is now with the School of Electrical and Computer Engineering, Cornell University, Ithaca, NY 14853 USA (e-mail: jaeweon.cho@ieee.org).

D. Hong is with the Department of Electronic Engineering, Sogang University, Seoul 121-742, Korea (e-mail: dhong@sogang.ac.kr).

Digital Object Identifier 10.1109/TWC.2003.821134

[1]In this paper, we refer to a set of data rates supported by physical channel as *a limited data rate set*.

level analysis [3]. Airy and Rohani [6] showed that the downlink throughput increases with the number of simultaneous users. The presented results in [6] are, however, not sufficient to show the effects of the self-interference and the limited data rate set on the system throughput.

The limitation of available spreading codes also should be considered for the exact evaluation of throughput. As downlink orthogonality gets higher, both the multi-user interference and the self-interference are decreased, and then the system throughput may be determined by the limited number of spreading codes. The available number of spreading codes in either VSF systems or MC systems should be restricted in order to maintain orthogonality [7]. Furukawa [8] showed that the spreading code shortage can affect the capacity of circuit data users. Likewise, packet data throughput can be limited by the available number of spreading codes.

This paper compares system throughput of CDM with that of time division multiplexing (TDM) on the multirate CDMA downlinks. We develop an analytical model and methodology that can reflect the effect of self-interference, the limited data rate set, and the shadowed radio paths. The limited number of spreading codes is also taken into account. In the next section, we set the system model in consideration of various features of the CDMA downlink. In Section III, we develop an analytical method for the system performance evaluation. The comparison results of CDM and TDM in a 3GPP WCDMA frequency-division duplex (FDD) system model are presented in Section IV. Finally, we draw conclusions in Section V.

II. System Model

We first formalize the problem of comparing CDM with TDM. Next, power allocation and data rate assignment in the system model is described. We propose the received bit energy per noise and interference power density (E_b/N_t) model including the impact of self-interference. The statistical model of the relative other cell interference is developed with considering the best BS selection. We also formulate the distribution of users being connected to a BS.

A. Problem Formalization of Comparing CDM With TDM

The packet transmissions with CDM and with TDM are hereafter called code-division scheduling (CDS) and time-division scheduling (TDS), respectively, as in [1]. The combined scheme can be applied by adjusting the number of the CDM users N, i.e., the number of users receiving simultaneously on downlink. The multiplexing and scheduling scheme with $N = 1$ can be regarded as pure TDS. As N is increased, the scheme works more as CDS.

The objective of this paper is to compare CDS with TDS in terms of the system throughput. This paper focuses on various features of the CDMA downlink, rather than the characteristics of the bursty traffic, such as the self-interference, the limited data rate set, the shadowed radio paths, and the location-dependent C/I. Hence, we assume a system with fully loaded cells where a number of users have data to send all the time, i.e., more than N users are waiting for receiving packets. Consequently, the problem to be solved in this work is a comparison of the asymptotic throughput for various settings of N.

B. Downlink Packet Transmission

The downlink in the system model is comprised of three channel types: overhead channel, circuit channel, and packet channel. Overhead channel is used to broadcast control information within a cell. All BSs have the same maximum transmission power P^M. A fixed portion α of P^M, i.e., P^O, is allocated to the overhead channels. For simplicity, total power of all the circuit channels for delay sensitive services is assumed to be a fixed portion δ of the current total BS transmission power P_i^C, i.e., $P_i^{Ckt} = \delta P_i^C$. Then, P_i^C can be represented by

$$P_i^C = \sum_{j=0}^{N-1} \beta_{i,j} P_{i,j}^U + P^O + P_i^{Ckt} \tag{1}$$

where the subscripts i and j denote the ith BS (BS_i) and the jth mobile station (MS_j), respectively. $P_{i,j}^U$ is the maximum allowable power for the MS_j, $\beta_{i,j}$ denotes the actual portion of $P_{i,j}^U$ for transmission $(0 < \beta_{i,j} \leq 1)$, and N is the number of data users receiving simultaneously.

The packet channel carries dedicated user data for delay tolerant services. We apply the simple power allocation scheme such that the remaining BS power after allocating P^O and P_i^{Ckt} is equally divided among packet data users receiving simultaneously. Therefore, $P_{i,j}^U$ for every user is the same as

$$P_{i,j}^U = P_i^U = \frac{P^M - P^O - P_i^{Ckt}}{N}. \tag{2}$$

The assigned data rate to a user is dependent on the received C/I. The highest available data rate is assigned to each user as long as the received E_b/N_t is maintained above the required value with the given power P_i^U. A rate control scheme can be applied to moving users, and it permits a data rate change in every frame [9]. The fast closed-loop power control is also applied to the packet channels [1], [10]. While the rate control scheme may assign a different data rate frame by frame according to the user location, the power control adjusts the transmission power slot by slot to achieve the E_b/N_t target. We assume the received E_b/N_t to be kept at its target by the perfect operation of the power control and the rate control. If any rate cannot be assigned because of a poor radio condition, an outage event occurs. When the outage occurs, the transmission opportunity and the power can be reallocated to another user having a good radio condition.

We illustrate the power and rate assignment with an example in Fig. 1. In the nth frame, the data rate $R1$ is assigned to a user, because P_i^U is lower than the required power for $R2$ but higher than that for $R1$. Note that P_i^U is the maximum allowable level for the averaged transmission power per frame. In the figure, the dotted line denotes the instantaneous power level that is adjusted by the fast power control. N_s denotes the number of slots per frame. The averaged transmission power over the nth frame becomes $\beta_{i,j} P_i^U$ due to the power control operation. Hence, the averaged transmission power per frame is always equal to or smaller than P_i^U.

An ideal automatic retransmission query (ARQ) procedure is assumed as follows: ARQ mechanism ensures retransmission of transport blocks in error, the number of repeat is unlimited, and the error rate of transport block, i.e., block-error rate (BLER), is kept at the required value by the power control and the rate control.

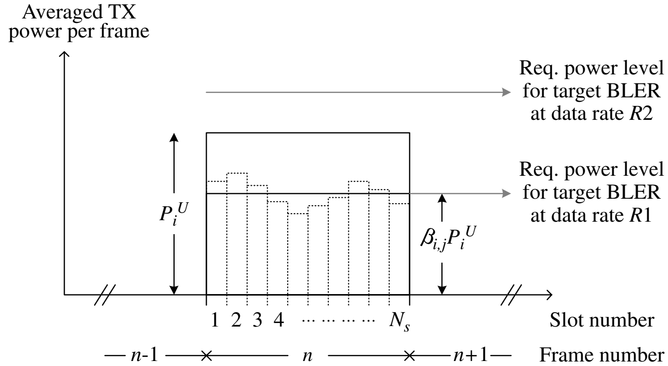

Fig. 1. Example of the power and rate assignment.

C. Received E_b/N_t Model

We propose the simple received E_b/N_t model including the impact of self-interference. In order to analyze the system performance with the effect of the self-interference, we should apply the different E_b/N_t targets to each data rate even though each one requires the same BLER. However, a complex link level analysis is needed for obtaining a large set of E_b/N_t targets. Hence, we need a more convenient way to take into consideration the effect of the self-interference. If performance of a forward-error correction (FEC) code, interleaving, and channel estimation is assumed to be identical for all date rates, we can simply but effectively model the received E_b/N_t reflecting the effect of the self-interference. Our proposed model does not require the large set of E_b/N_t targets for the whole data rates, but only one E_b/N_t target for the lowest data rate. This model is also applicable to both VSF systems and MC systems.

For the MC system, considered the self-interference between MC channels, the received E_b/N_t of a code channel can be modeled as follows:

$$\left(\frac{E_b}{N_t}\right)_{i,j} = \frac{\beta_{i,j}P_{i,j}^{Code}}{I_{i,j}^{SF}+I_{i,j}^{SC}+I_{i,j}^{OC}}\cdot\frac{W}{R_0} \tag{3}$$

where spreading bandwidth W is assumed to be the chip rate and R_0 denotes the data rate of a code channel. The maximum allowable power per code channel $P_{i,j}^{Code}$ is given by

$$P_{i,j}^{Code} = \frac{P_i^U}{k_{i,j}} \tag{4}$$

where $k_{i,j}$ is the number of the assigned MC channels. The maximum $k_{i,j}$ satisfying the following condition is assigned to a user:

$$\frac{\frac{\beta_{i,j}P_i^U}{k_{i,j}}}{I_{i,j}^{SF}+I_{i,j}^{SC}+I_{i,j}^{OC}}\cdot\frac{W}{R_0} \ge \left(\frac{E_b}{N_t}\right)_{\mathrm{REQ}} \tag{5}$$

where $(E_b/N_t)_{\mathrm{REQ}}$ is the required value for a target BLER at the data rate R_0. Then, the aggregate data rate for the user $R_{i,j}$ is given by

$$R_{i,j} = k_{i,j}\cdot R_0. \tag{6}$$

Total interference can be divided into the self-interference $I_{i,j}^{SF}$, same cell interference $I_{i,j}^{SC}$, and other cell interference $I_{i,j}^{OC}$. In (3), thermal noise is assumed to be negligible. $I_{i,j}^{SF}$ denotes the interference between MC channels assigned to a user. Hence, it is proportional to $k_{i,j}$. $I_{i,j}^{SC}$ is the sum of the interferences from the other packet channels, overhead channels, and circuit channels within the same cell. $I_{i,j}^{OC}$ is the total interference from other BSs. These can be expressed as

$$I_{i,j}^{SF} = (1-\phi^{SF})\beta_{i,j}(k_{i,j}-1)P_{i,j}^{Code} \tag{7}$$

$$I_{i,j}^{SC} = (1-\phi^{SC})\left(\sum_{n=0,n\neq j}^{N-1}\beta_{i,n}P_{i,n}^U + P^O + P_i^{Ckt}\right) \tag{8}$$

$$I_{i,j}^{OC} = \sum_{m=0,m\neq i}^{M}\sum_{n=0}^{N-1}\left(\beta_{m,n}P_{m,n}^U + P^O + P_m^{Ckt}\right)\frac{L_{m,j}}{L_{i,j}} \tag{9}$$

where M is the number of BSs near BS_i.

In (7) and (8), ϕ^{SF} and ϕ^{SC} denote orthogonality between MC channels. An orthogonality factor of 1 corresponds to perfectly orthogonal code channels, while with the factor of 0 the orthogonality is lost. Link level study [3] showed that the lack of orthogonality between code channels of a user is similar to that between other user code channels. Therefore, the two values can be approximated to be identical as

$$\phi \approx \phi^{SF} \approx \phi^{SC}. \tag{10}$$

In (9), $L_{i,j}$ denotes the path gain. At distance $r_{i,j}$ from BS_i, the propagation loss is inversely proportional to

$$L_{i,j} = r_{i,j}^{-\mu}10^{\frac{(a\hat{\xi}_j+b\xi_i)}{10}} \tag{11}$$

where μ is the path loss exponent. $\hat{\xi}_j$ and ξ_i are the MS_j shadowing and the BS_i shadowing, respectively. They both are *Gaussin* random variables with zero mean and standard deviation σ. In this model, site to site correlation is applied as $a^2 = 1-b^2$ [11].

The E_b/N_t model shown previously can also be applied to the VSF system because it was reported that the link level performance with the VSF scheme is approximately equal to that with the MC scheme [3]. For the VSF systems, the minimum data rate R_0 should be set to the data rate for the largest SF. Then, R_0 and $k_{i,j}$ can be regarded as the data rate of an equivalent code channel and the number of the assigned equivalent code channels, respectively. Note that $k_{i,j}$ for VSF systems is a power of 2 because SF in most systems is given by a power of 2.

D. Statistical Model of the Relative Other Cell Interference

We show a statistical model of the downlink interference for the analytical performance evaluation. The received E_b/N_t on the CDMA downlink is mainly influenced by the ratio of interference from adjacent BS to that from the connected BSs. MS in the shadowed environment is connected to the BS with the smallest propagation loss, i.e., the best BS, rather than the closest BS. The best BS selection can considerably affect the statistics of the relative interference. Pratesi *et al.* [12] analyzed the cochannel interference statistics with various methods but without considering the best BS selection. In this work, based on *Wilkinson's* approximation that is one of the well-known log-normal approximations [12], [13], the statistical model of the relative other cell interference is developed with considering the best BS selection.

We define random variables X and Z as

$$X_{i,j} \equiv \sum_{m=0,m\neq i}^{M} \frac{L_{m,i}}{L_{i,j}} = \sum_{m=0,m\neq i}^{M} Y_{i,m,j} \tag{12}$$

$$Z_{i,j} \equiv 10 \log X_{i,j} \tag{13}$$

where $Y_{i,m,j} \equiv L_{m,i}/L_{i,j} = V_{i,m,j} 10^{b(\xi_m - \xi_i)/10}$ and $V_{i,m,j} \equiv (r_{i,j}/r_{m,j})^{\mu}$. Note that the distance from BS_m to MS_j, $r_{m,j}$ can be represented by a function of $(r_{i,j}, \theta_{i,j})$, which are the polar coordinates with respect to BS_i. The subscripts of $(r_{i,j}, \theta_{i,j})$ are, hereafter, dropped for convenience, i.e., $r \equiv r_{i,j}$ and $\theta \equiv \theta_{i,j}$. Note that $V_{i,m,j}$ also can be represented by a function of (r, θ).

The first and the second moments of X at the given position (r, θ) can be obtained as

$$m_{X_{i,j}|r,\theta} \equiv E[X_{i,j}|r,\theta] = \sum_{\substack{m=0 \\ m\neq i}}^{M} E[Y_{i,m,j}|r,\theta] \tag{14}$$

$$\begin{aligned} \nu_{X_{i,j}|r,\theta} &\equiv E\left[X_{i,j}^2|r,\theta\right] \\ &= \sum_{\substack{m=0 \\ m\neq i}}^{M} E\left[Y_{i,m,j}^2|r,\theta\right] \\ &\quad + \sum_{\substack{l=0 \\ l\neq i}}^{M} \sum_{\substack{m=0 \\ m\neq i \\ m\neq l}}^{M} E[Y_{i,l,j} Y_{i,m,j}|r,\theta]. \end{aligned} \tag{15}$$

With the best BS selection, every MS is connected to the BS with the smallest propagation loss. Therefore, the inequality $L_{i,j} > L_{m,j}$ should be met for all m except i in (12). If without the condition $L_{i,j} > L_{m,j}$, the shadowing random variables of BS ξs are independent with one another, then their joint probability density function (PDF) can be represented by

$$\begin{aligned} f_{\underline{\xi}}(\underline{\xi}) &= f_{\xi_0,\xi_1,\cdots,\xi_M}(\xi_0, \xi_1, \cdots, \xi_M) \\ &= \prod_{n=0}^{M} f_{\xi_n}(\xi_n) = \prod_{n=0}^{M} \frac{1}{\sqrt{2\pi}\sigma} e^{-\frac{\xi_n^2}{2\sigma^2}}. \end{aligned} \tag{16}$$

By using (16), the excepted value in (14) with the condition $L_{i,j} > L_{m,j}$ can be computed as in (17), shown at the bottom of the page, where $A_{i,n,j}(x,y)$ is defined by using the error function $\mathrm{erf}(\cdot)$ as

$$A_{i,n,j}(x,y) \equiv \frac{1}{2} + \frac{1}{2}\mathrm{erf}\left(\frac{bx - 10\log V_{i,n,j}}{\sqrt{2}b\sigma} - y\frac{\sigma b \ln 10}{10\sqrt{2}}\right). \tag{18}$$

Note that $A_{i,n,j}(x,y)$ depends on (r,θ) because $V_{i,m,j}$ is a function of (r,θ). Although $A_{i,n,j}(x,y,r,\theta)$ is the exact notation, $A_{i,n,j}(x,y)$ is used for convenience.

In similar way, the expected values in (15) can be derived as in (19) and (20), shown at the bottom of the page.

As the conventional *Wilkinson's* approximation, we approximate X as a log-normal random variable. Z then becomes a *Gaussian* random variable with mean $m_{Z_{i,j}|r,\theta} = 10\log(m_{X_{i,j}|r,\theta}^2/\sqrt{\nu_{X_{i,j}|r,\theta}})$ and variance $\sigma_{Z_{i,j}|r,\theta}^2 = (100/\ln 10)\log(\nu_{X_{i,j}|r,\theta}/m_{X_{i,j}|r,\theta}^2)$ [13]. Zorzi [14] provided the joint PDF of $L_{i,j}$ for $i = 0, 1, \cdots, M$, considering the

$$\begin{aligned} E[Y_{i,m,j}|r,\theta] &= \int V_{i,m,j} 10^{\frac{b(x_m - x_i)}{10}} f_{\underline{\xi}}\left(\underline{x}|(r,\theta),(L_{i,j} > L_{0,j}, L_{i,j} > L_{1,j}, \cdots, L_{i,j} > L_{M,j})\right) d\underline{x} \\ &= V_{i,m,j} \frac{\int_{-\infty}^{\infty} 10^{-\frac{bx_i}{10}} f_{\xi_i}(x_i) \int_{-\infty}^{x_i - \frac{10}{b}\log V_{i,m,j}} 10^{\frac{bx_m}{10}} f_{\xi_m}(x_m) dx_m \prod_{n=0,n\neq i,n\neq m}^{M} \left[\int_{-\infty}^{x_i - \frac{10}{b}\log V_{i,n,j}} f_{\xi_n}(x_n) dx_n\right] dx_i}{\int_{-\infty}^{\infty} f_{\xi_i}(x_i) \prod_{n=0,n\neq i}^{M} \left[\int_{-\infty}^{x_i - \frac{10}{b}\log V_{i,n,j}} f_{\xi_n}(x_n) dx_n\right] dx_i} \\ &= V_{i,m,j} e^{\frac{\sigma^2 b^2 (\ln 10)^2}{200}} \cdot \frac{\int_{-\infty}^{\infty} 10^{-\frac{bx}{10}} e^{-\frac{x^2}{2\sigma^2}} A_{i,m,j}(x,1) \prod_{n=0,n\neq i,n\neq m}^{M} A_{i,n,j}(x,0) dx}{\int_{-\infty}^{\infty} e^{-\frac{x^2}{2\sigma^2}} \prod_{n=0,n\neq i}^{M} A_{i,n,j}(x,0) dx} \end{aligned} \tag{17}$$

$$\begin{aligned} E\left[Y_{i,m,j}^2|r,\theta\right] &= V_{i,m,j}^2 e^{\frac{\sigma^2 b^2 (\ln 10)^2}{50}} \\ &\quad \cdot \frac{\int_{-\infty}^{\infty} 10^{-\frac{bx}{5}} e^{-\frac{x^2}{2\sigma^2}} A_{i,m,j}(x,2) \prod_{n=0,n\neq i,n\neq m}^{M} A_{i,n,j}(x,0) dx}{\int_{-\infty}^{\infty} e^{-\frac{x^2}{2\sigma^2}} \prod_{n=0,n\neq i}^{M} A_{i,n,j}(x,0) dx} \end{aligned} \tag{19}$$

$$\begin{aligned} E[Y_{i,l,j} Y_{i,m,j}|r,\theta] &= V_{i,l,j} V_{i,m,j} e^{\frac{\sigma^2 b^2 (\ln 10)^2}{100}} \\ &\quad \cdot \frac{\int_{-\infty}^{\infty} 10^{-\frac{bx}{5}} e^{-\frac{x^2}{2\sigma^2}} A_{i,l,j}(x,1) A_{i,m,j}(x,1) \cdot \prod_{n=0,n\neq i,n\neq m,n\neq l}^{M} A_{i,n,j}(x,0) dx}{\int_{-\infty}^{\infty} e^{-\frac{x^2}{2\sigma^2}} \prod_{n=0,n\neq i}^{M} A_{i,n,j}(x,0) dx} \end{aligned} \tag{20}$$

best BS selection. From the provided formula, however, it is not easy to obtain the PDF of X or Z in closed form. In our approach, though the log-normal approximation is employed and numerical integrations are involved, the PDF of Z has been obtained in the closed form of normal distribution that would be very useful for system-level analyses.[2]

E. Distribution of the Connected Users

We formulate the distribution of MSs that have been successfully connected to the BS of interest. As explained, MS is connected to the BS with the smallest propagation loss rather than the closest BS. For the exact analysis, we should use the MS distribution including the effect of the best BS selection.

Let $f(r,\theta|\mathrm{BS}_i,\mathrm{Avail})$ be the conditional joint PDF of (r,θ) on the condition that MS, having been located at (r,θ), is connected to the BS_i and its radio link is available. This PDF can be derived as in (21), shown at the bottom of the page, where $\Pr(\mathrm{BS}_i,\mathrm{Avail}|r,\theta)$ is the probability that MS, having been located at (r,θ), is connected to the BS_i and the radio link is available. $\Pr(\mathrm{Out}|\mathrm{BS}_i,(r,\theta))$ is outage probability for the MS having selected BS_i at (r,θ). A_0 denotes the entire region that is feasible for the selection of BS_i. $f(r,\theta)$ is the joint PDF of the MS position on the region A_0, regardless of the connected BS.

The probability of selecting BS_i at the given position (r,θ) is computed as

$$\begin{aligned}\Pr(\mathrm{BS}_i|r,\theta) &= \Pr(L_{i,j} > L_{0,j},\cdots,L_{i,j} > L_{M,j}|r,\theta)\\ &= \frac{1}{\sqrt{2\pi}\sigma}\int_{-\infty}^{\infty} e^{-\frac{x^2}{2\sigma^2}} \prod_{n=0,n\neq i}^{M} A_{i,n,j}(x,0)dx. \end{aligned} \tag{22}$$

Note that $A_{i,n,j}(x,0)$ depends on (r,θ), as explained in the previous subsection.

The distribution of the connected users $f(r,\theta|\mathrm{BS}_i,\mathrm{Avail})$ can be computed by using (21), (22), the given distribution $f(r,\theta)$, and $\Pr(\mathrm{Out}|\mathrm{BS}_i,(r,\theta))$ that will be formulated in the next section.

III. Performance Analysis

We develop an analytical method for throughput analysis in the shown environment. First, the distribution of the data rate assigned to a user is derived by using the developed analytical models. Next, we define and derive various system performance measures: outage probability, probability of the data rate being limited by the given rate set, code shortage probability, and asymptotic throughput.

[2]In regard to validation of the applied approximation, see [15].

A. Distribution of the Assigned Data Rate

To begin with, let us define $p_R(R|\mathrm{BS}_i,\mathrm{Avail})$ as the distribution of the data rate assigned to a user who has selected BS_i and had an available radio link. The subscripts i and j are dropped for convenience. Since $R = k\cdot R_0$, $p_R(R|\mathrm{BS}_i,\mathrm{Avail})$ is derived in the form of probability mass function (PMF), and also it is identical to the conditional PMF of k, $p_k(k|\mathrm{BS}_i,\mathrm{Avail})$. We can obtain $p_k(k|\mathrm{BS}_i,\mathrm{Avail})$ by averaging the PMF of each position over the region A_0. Therefore

$$p_k(k|\mathrm{BS}_i,\mathrm{Avail}) = \iint_{A_0} p_k(k|\Xi)\cdot f(r,\theta|\mathrm{BS}_i,\mathrm{Avail})drd\theta \tag{23}$$

where the event $\Xi \equiv ((r,\theta),\mathrm{BS}_i,\mathrm{Avail})$ means that user is located at (r,θ), selects BS_i, and has an available radio link. The PDF $f(r,\theta|\mathrm{BS}_i,\mathrm{Avail})$ was formulated in previous section. Hence, we have only to derive the conditional PMF $p_k(k|\Xi)$. The goal of this subsection is to obtain $p_k(k|\Xi)$.

We begin by simplifying the received E_b/N_t expression so that k can be represented as a simple function of *Gaussian* random variable Z. Then, we obtain $p_k(k|\Xi)$ from the PDF of Z. We also derive the outage probability and the probability of the data rate being limited by the given rate set.

1) Simplification of the Received E_b/N_t: We first simplify the expression of the maximum allowable power for data user, i.e., P_i^U in (2). Let us assume random variable $\beta_{i,j}$ in (1) to be a constant value $\bar{\beta}$, which is to be defined and derived in the next subsection. Then, P_i^{Ckt} and P_i^U can be represented by P^{Ckt} and P^U, respectively

$$P_i^{Ckt} \approx P^{Ckt} \equiv \zeta P^M \tag{24}$$

$$P_i^U \approx P^U \equiv \frac{1-\alpha-\zeta}{N}P^M \tag{25}$$

where

$$\zeta \equiv \frac{\delta\left[\alpha(1-\bar{\beta})+\bar{\beta}\right]}{1-\delta(1-\bar{\beta})}. \tag{26}$$

We now consider the received E_b/N_t expression in (5). Every BS tries to make the utmost use of the given power P^U in order to assign a higher data rate. Therefore, β for the user of interest in (5) and (7), i.e., $\beta_{i,j}$, should be set to 1. On the other hand, βs for other users in (8) and (9), i.e., $\beta_{i,n}$ and $\beta_{m,n}$, are assumed to be $\bar{\beta}$ for simplicity.[3]

[3]The setting of $\beta_{i,j}=1$ is valid only when we find the maximum $k_{i,j}$ satisfying (5). It is because the given power P^U should be utilized to the fullest for the highest possible $k_{i,j}$. However, since $k_{i,j}$ is a discrete value with a peak limitation, the actual transmission power after determining $k_{i,j}$ becomes lower than P^U, as shown in Fig. 1. When computing interference from other user signals, we should consider the actual transmission power. For this reason, we assume that β for the other user is a constant smaller than 1.

$$\begin{aligned} f(r,\theta|\mathrm{BS}_i,\mathrm{Avail}) &= \frac{\Pr(\mathrm{BS}_i,\mathrm{Avail}|r,\theta)\cdot f(r,\theta)}{\iint_{A_0}\Pr(\mathrm{BS}_i,\mathrm{Avail}|r,\theta)\cdot f(r,\theta)drd\theta}\\ &= \frac{\Pr\left(\mathrm{Avail}|\mathrm{BS}_i,(r,\theta)\right)\cdot\Pr(\mathrm{BS}_i|r,\theta)\cdot f(r,\theta)}{\iint_{A_0}\Pr\left(\mathrm{Avail}|\mathrm{BS}_i,(r,\theta)\right)\cdot\Pr(\mathrm{BS}_i|r,\theta)\cdot f(r,\theta)drd\theta}\\ &= \frac{\left[1-\Pr\left(\mathrm{Out}|\mathrm{BS}_i,(r,\theta)\right)\right]\cdot\Pr(\mathrm{BS}_i|r,\theta)\cdot f(r,\theta)}{\iint_{A_0}\left[1-\Pr\left(\mathrm{Out}|\mathrm{BS}_i,(r,\theta)\right)\right]\cdot\Pr(\mathrm{BS}_i|r,\theta)\cdot f(r,\theta)drd\theta} \end{aligned} \tag{21}$$

We are to represent the discrete random variable k as a function of the *Gaussian* random variable Z. Since Z is a continuous value, we need to introduce the continuous random variable of k. Let the continuous random variable of k be $\tilde{k}$. We may then replace k with $\tilde{k}$ in (5) and invert (5) as an equality. Next, substitute P^{Ckt} for P_i^{Ckt} and P_m^{Ckt} and P^U for P_i^U, and P_m^U. Then, solving (5) for $\tilde{k}$, we have

$$\tilde{k} = g(Z) \equiv \frac{\Lambda}{\Gamma + 10^{\frac{Z}{10}}} \tag{27}$$

where

$$\Lambda \equiv \frac{(1-\alpha-\zeta)\left[(1-\phi) + \frac{\left(\frac{W}{R_0}\right)}{\left(\frac{E_b}{N_t}\right)_{\mathrm{REQ}}}\right]}{N\left[(1-\alpha-\zeta)\bar{\beta} + \alpha + \zeta\right]} \tag{28}$$

$$\Gamma \equiv \frac{(1-\phi)\left[(1-\alpha-\zeta)\left(\bar{\beta} + \frac{(1-\bar{\beta})}{N}\right) + \alpha + \zeta\right]}{(1-\alpha-\zeta)\bar{\beta} + \alpha + \zeta}. \tag{29}$$

Therefore, k in the VSF systems can be represented by

$$k = 2^{\lfloor \log_2 \tilde{k} \rfloor} = 2^{\lfloor \log_2 g(Z) \rfloor} \tag{30}$$

where $\lfloor x \rfloor$ denotes the largest integer that is smaller than or equal to x.[4] Considered the peak data rate limitation, its maximum can be set to

$$k_{\max} \equiv \min\left(\frac{R_{\max}}{R_0}, 2^{\left\lfloor \lim_{Z \to -\infty} \tilde{k} \right\rfloor}\right) = \min\left(\frac{R_{\max}}{R_0}, 2^{\left\lfloor \log_2 \frac{\Lambda}{\Gamma} \right\rfloor}\right) \tag{31}$$

where $R_{\max}$ is the maximum allowable data rate per packet channel.

2) Distribution of the Data Rate Assigned to a User: In this tertiary section, we derive the distribution of k by using (27) and the PDF of Z. Since $p_k(k|\Xi)$ is for the user having an available radio link, we must consider Z for the nonoutage user.

As explained earlier, we apply an outage handling scheme that reallocates transmission opportunity of an outage user to another user having a good radio condition. The outage events occur when $\tilde{k}$ is smaller than 1. From (27), this outage condition can be rewritten as $Z > Z_{\max} \equiv 10\log(\Lambda - \Gamma)$. Therefore, Z for the nonoutage user can be defined as $\hat{Z}$ such that $-\infty < \hat{Z} \le Z_{\max}$. Its PDF, then, is

$$f_{\hat{Z}}(z) = f_Z(z|z \le Z_{\max}) = \begin{cases} \frac{\varepsilon}{\sqrt{2\pi}\sigma_{Z|r,\theta}} \times \exp\left(-\frac{(z-m_{Z|r,\theta})^2}{2\sigma_{Z|r,\theta}^2}\right), & \text{for } z \le Z_{\max} \\ 0, & \text{for } z > Z_{\max} \end{cases} \tag{32}$$

where

$$\varepsilon \equiv \frac{2}{1 + \mathrm{erf}\left(\frac{Z_{\max} - m_{Z|r,\theta}}{\sqrt{2}\sigma_{Z|r,\theta}}\right)}. \tag{33}$$

Note that $f_{\hat{Z}}(z)$ and $f_Z(z)$ should be regarded as the conditional PDFs, given the event of $((r,\theta), \mathrm{BS}_i)$, because both $\hat{Z}$ and Z are for the user that has been located at (r,θ) and connected to BS_i. Although $f_{\hat{Z}}(z|(r,\theta),\mathrm{BS}_i)$ and $f_Z(z|(r,\theta),\mathrm{BS}_i)$ are the exact notations, we drop $((r,\theta),\mathrm{BS}_i)$ just for convenience. Note that ε is also a function of (r,θ) because $m_{Z|r,\theta}$ and $\sigma_{Z|r,\theta}$ depend on (r,θ).

We now derive the PMF of k from the PDF of $\tilde{k}$. Considering the applied outage handling scheme, we replace Z with $\hat{Z}$ in (27). Since $\tilde{k}$ is a function of $\hat{Z}$, the PDF of $\tilde{k}$ can be obtained from $f_{\hat{Z}}(z)$ as follows [16]:

$$f_{\tilde{k}}(\tilde{k}|\Xi) = \frac{f_{\hat{Z}}(\hat{z})}{|g'(\hat{z})|} = \frac{10 \cdot \Lambda \cdot \varepsilon}{\sqrt{2\pi} \cdot \ln 10 \cdot \sigma_{Z|r,\theta} \cdot \tilde{k}^2 \cdot \left(\frac{\Lambda}{\tilde{k}} - \Gamma\right)} \cdot \exp\left(-\frac{\left(10\log\left(\frac{\Lambda}{\tilde{k}} - \Gamma\right) - m_{Z|r,\theta}\right)^2}{2\sigma_{Z|r,\theta}^2}\right). \tag{34}$$

Therefore, the PMF of k can be computed as

$$p_k(k|\Xi) = \begin{cases} \int_k^{\frac{\Lambda}{\Gamma}} f_{\tilde{k}}(\tilde{k}|\Xi)d\tilde{k}, & \text{for } k = k_{\max} \\ \int_k^{2k} f_{\tilde{k}}(\tilde{k}|\Xi)d\tilde{k}, & \text{for } 1 \le k < k_{\max} \end{cases} \tag{35}$$

where the integration can be computed by using the error functions as follows:

$$\int_{\eta_1}^{\eta_2} f_{\tilde{k}}(x|\Xi)dx = \frac{\varepsilon}{2}\left[\mathrm{erf}\left(\frac{m_{Z|r,\theta} - 10\log\left(\frac{\Lambda}{\eta_2} - \Gamma\right)}{\sqrt{2}\sigma_{Z|r,\theta}}\right) - \mathrm{erf}\left(\frac{m_{Z|r,\theta} - 10\log\left(\frac{\Lambda}{\eta_1} - \Gamma\right)}{\sqrt{2}\sigma_{Z|r,\theta}}\right)\right]. \tag{36}$$

Consequently, the distribution of the assigned data rate $p_R(R|\mathrm{BS}_i, \mathrm{Avail})$ can be obtained by using (21), (23), and (35).

3) Outage Probability: Outage probability at each position is given by

$$\Pr(\mathrm{Out}|(r,\theta),\mathrm{BS}_i) = \Pr(Z > Z_{\max}|(r,\theta),\mathrm{BS}_i) = 1 - \frac{1}{\varepsilon}. \tag{37}$$

Outage probability P_{Out} is defined as the averaged outage probability over the region A_0, and it can be computed as

$$P_{\mathrm{Out}} = \iint_{A_0} \Pr(\mathrm{Out}|(r,\theta),\mathrm{BS}_i) \cdot f(r,\theta|\mathrm{BS}_i) dr d\theta \tag{38}$$

where $f(r,\theta|\mathrm{BS}_i)$ is computed by using $\Pr(\mathrm{BS}_i|r,\theta)$ and $f(r,\theta)$ in similar way to obtain $f(r,\theta|\mathrm{BS}_i, \mathrm{Available})$ in (21).

4) Probability of the Data Rate Being Limited by the Given Rate Set: Here, we derive the probability P_{UL} that the data rate assigned to a user is determined by the peak data rate limitation. Let $\Pr(UL|\Xi)$ be the conditional probability of P_{UL} at each position. Then, $\Pr(UL|\Xi)$ can be defined as the probability of $\tilde{k} \ge 2k_{\max}$ given the event of Ξ, and it can be computed as

$$\Pr(UL|\Xi) \equiv \int_{2k_{\max}}^{\Lambda/\Gamma} f_{\tilde{k}}(\tilde{k}|\Xi)d\tilde{k} = \frac{\varepsilon}{2}\left[1 - \mathrm{erf}\left(\frac{m_{Z|r,\theta} - 10\log\left(\frac{\Lambda}{2k_{\max}} - \Gamma\right)}{\sqrt{2}\sigma_{Z|r,\theta}}\right)\right]. \tag{39}$$

[4]In the MC systems, k can be represented as $k = \lfloor \tilde{k} \rfloor = \lfloor g(Z) \rfloor$.

Note that the quantization of $\tilde{k}$ for $k_{\max} \leq \tilde{k} < 2k_{\max}$ to $k_{\max}$ is due to the granularity of the data rate rather than the peak data rate limitation. Therefore, the lower bound on the previous integration is set to $2k_{\max}$. By using $\Pr(UL|\Xi)$, P_{UL} can be represented as

$$P_{UL} = \iint_{A_0} \Pr(UL|\Xi) \cdot f(r,\theta|\mathrm{BS}_i, \mathrm{Avail}) dr d\theta. \quad (40)$$

The performance measures P_{UL} and P_{Out} are useful to show the effect of the limited data rate set on throughput, which will be presented in the next section.

B. Power Usage Efficiency per User

The power usage efficiency per user $\bar{\beta}$ is needed for computation of the $p_R(R|\mathrm{BS}_i, \mathrm{Avail})$. Recall that the given P_i^U cannot always be exhausted because of the data rate granularity, the peak data rate limitation, and the power control operation. Therefore, its actual portion for transmission β is smaller than or equal to one. The power usage efficiency $\bar{\beta}$ is defined as the expected value of β.

At each position, β can be represented by a function of $\hat{Z}$. First, invert (5) as an equality and assume βs for other users in (8) and (9), i.e., $\beta_{i,n}$ and $\beta_{m,n}$ to be $\bar{\beta}$. Next, substitute P^{Ckt} for P_i^{Ckt} and P_m^{Ckt}, and P^U for P_i^U and P_m^U. Then, solving (5) for $\beta_{i,j}$ and dropping the subscripts, we get

$$\beta = q(\hat{Z}) \cdot \left(\Psi + 10^{\frac{\hat{Z}}{10}}\right) \quad (41)$$

where

$$\Psi \equiv \frac{(1-\phi)\left[\bar{\beta}(1-\alpha-\zeta)\left(1-\frac{1}{N}\right)+\alpha+\zeta\right]}{\bar{\beta}(1-\alpha-\zeta)+\alpha+\zeta} \quad (42)$$

$$q(\hat{Z}) \equiv \frac{2^{\lfloor \log_2 g(\hat{Z}) \rfloor} \cdot N \cdot \left(\frac{E_b}{N_t}\right)_{\mathrm{REQ}}}{1-\alpha-\zeta} \cdot \frac{\bar{\beta}(1-\alpha-\zeta)+\alpha+\zeta}{\frac{W}{R_0} - (1-\phi)\left(2^{\lfloor \log_2 g(\hat{Z}) \rfloor} - 1\right)\left(\frac{E_b}{N_t}\right)_{\mathrm{REQ}}}. \quad (43)$$

The expected value of β at (r,θ), $E[\beta|\Xi]$ can be obtained by using $f_{\hat{Z}}(\hat{z})$

$$\begin{aligned} E[\beta|\Xi] &= \int_{-\infty}^{Z_{\max}} \beta \cdot f_{\hat{Z}}(\hat{z}) d\hat{z} \\ &= \int_{-\infty}^{Z_{\max}} q(\hat{z}) \cdot \left(\Psi + 10^{\frac{\hat{z}}{10}}\right) \cdot f_{\hat{Z}}(\hat{z}) d\hat{z}. \quad (44) \end{aligned}$$

Since the quantized value k is given by $2^{\lfloor \log_2 g(\hat{Z}) \rfloor}$, k and $q(\hat{Z})$ are constant for a certain range of $\hat{Z}$. Therefore, the integration in (44) can be computed by subdividing the interval as

$$\begin{aligned} E[\beta|\Xi] = &\int_{-\infty}^{10\log\left(\frac{\Lambda}{k_{\max}}-\Gamma\right)} q(\hat{z}) \cdot \left(\Psi + 10^{\frac{\hat{z}}{10}}\right) \cdot f_{\hat{Z}}(\hat{z}) d\hat{z} + \cdots \\ &+ \int_{10\log\left(\frac{\Lambda}{2k}-\Gamma\right)}^{10\log\left(\frac{\Lambda}{k}-\Gamma\right)} q(\hat{z}) \cdot \left(\Psi + 10^{\frac{\hat{z}}{10}}\right) \cdot f_{\hat{Z}}(\hat{z}) d\hat{z} + \cdots \\ &+ \int_{10\log\left(\frac{\Lambda}{2}-\Gamma\right)}^{10\log(\Lambda-\Gamma)} q(\hat{z}) \cdot \left(\Psi + 10^{\frac{\hat{z}}{10}}\right) \cdot f_{\hat{Z}}(\hat{z}) d\hat{z}. \quad (45) \end{aligned}$$

Each integration term can be derived as follows:

$$\begin{aligned} \int_{\gamma_1}^{\gamma_2} & q(\hat{z}) \left(\Psi + 10^{\frac{\hat{z}}{10}}\right) \cdot f_{\hat{Z}}(\hat{z}) d\hat{z} \\ &= \frac{\varepsilon \cdot q(\gamma_2)}{2} \left[\Psi \left(B(\gamma_2, 0) - B(\gamma_1, 0)\right)\right. \\ &\quad + e^{m_{Z|r,\theta} \frac{\ln 10}{10} + \sigma_{Z|r,\theta}^2 \frac{(\ln 10)^2}{200}} \\ &\quad \left. \times \left(B(\gamma_2, 1) - B(\gamma_1, 1)\right)\right] \quad (46) \end{aligned}$$

where

$$B(x,y) \equiv \mathrm{erf}\left(\frac{x - m_{Z|r,\theta} - \frac{y\sigma_{Z|r,\theta}^2(\ln 10)}{10}}{\sqrt{2}\sigma_{Z|r,\theta}}\right). \quad (47)$$

By using the previous equations, we can compute $\bar{\beta}$ as

$$\bar{\beta} = \iint_{A_0} E[\beta|\Xi] \cdot f(r,\theta|\mathrm{BS}_i, \mathrm{Avail}) dr d\theta. \quad (48)$$

Since the integration in the right side involves $\bar{\beta}$ as well, it is not easy to find the exact solution in closed form. Fortunately, it can be solved by using a numerical method. Because the right-hand side can be represented as a function of $\bar{\beta}$, the previous equation can be rewritten as

$$S(\bar{\beta}) \equiv \bar{\beta} - \iint_{A_0} E[\beta|\Xi] \cdot f(r,\theta|\mathrm{BS}_i, \mathrm{Avail}) dr d\theta = 0. \quad (49)$$

We can find a solution $\bar{\beta}$ by applying an iteration method such as the *method of false position* to the equation $S(\bar{\beta}) = 0$ (see [17] for description of the *method of false position*).

C. System Throughput

The system throughput is defined and derived by using the assigned data rate distribution that has been obtained in the previous subsection. To simplify notation, we will write $p_R(R|\mathrm{BS}_i, \mathrm{Avail})$ as $p_R(R)$ in the following discussion.

We first derive the distribution of the total data rate transmitted by a BS. Even scheduling is applied so that the equal amount of service time is assigned to all users. The total data rate C is the sum of the assigned N data rates. For simplicity, we assumed these N data rates to be independent of one another. Note that the maximum of C, $C_{\max}$ may be smaller than $N \cdot R_{\max}$ because of the limited number of the downlink spreading codes. The characteristic function of C can be derived by using the *discrete Fourier transform* (DFT) and the *convolution theorem* [18]. We refer to the characteristic function of C as d_m and then can compute it as

$$\begin{aligned} d_m \equiv \Phi_C\left(\frac{2\pi m}{N \cdot n_{\max}}\right) &= \Phi_R\left(\frac{2\pi m}{N \cdot n_{\max}}\right)^N \\ &= \left[\sum_{l=0}^{\log_2(n_{\max})} R\left(2^l \cdot R_0\right) e^{\frac{j2\pi 2^l m}{N \cdot n_{\max}}}\right]^N \quad (50) \end{aligned}$$

where $m = 0, 2, \cdots, N \cdot n_{\max} - 1$ and $n_{\max} \equiv R_{\max}/R_0$. $\Phi_C(\cdot)$ and $\Phi_R(\cdot)$ denote the characteristic functions of C and

R, respectively. Then, the PMF of C can be recovered as in (51), shown at the bottom of page.

When C exceeds $C_{\max}$, the code shortage occurs and then C is limited to $C_{\max}$. Therefore, probability of the system throughput being limited by the available number of spreading codes, i.e., code shortage probability, can be given by

$$\begin{aligned} P_{SL} &\equiv \Pr(C > C_{\max}) \\ &= \sum_{n=\frac{C_{\max}}{R_0}+1}^{N\cdot n_{\max}} \left[\frac{1}{N\cdot n_{\max}} \sum_{m=0}^{N\cdot n_{\max}-1} d_m e^{-\frac{j2\pi nm}{N\cdot n_{\max}}} \right]. \end{aligned} \tag{52}$$

At last, we define asymptotic throughput as the expected value of the effective total data rate that a BS transmits at full loading. The effective data rate can be represented by using BLER as in [19]. Therefore

$$\begin{aligned} \text{Asymptotic throughput} &\equiv \frac{E[C]}{1+\sum_{i=1}^{\infty} \text{BLER}^i} \\ &= (1-\text{BLER}) \sum_{n=1}^{\frac{C_{\max}}{R_0}} n \cdot R_0 \\ &\quad \cdot p_C(n \cdot R_0). \end{aligned} \tag{53}$$

IV. Comparison Results

A. *Simple Comparison in the System With the Unlimited Data Rate Set*

Before proceeding to the performance analysis of the system with the limited data rate set, we compare the throughput of CDS with that of TDS in the system without the data rate limitation. In order to focus on the effect of the self-interference and the multi-user interference, we simplify the system model as follows: the downlink is comprised of only packet channels, i.e., $\alpha = \delta = 0$, and the data rate for the packet channel is continuous and unlimited. With this assumption, all βs can be set to one because the given power to every user is completely consumed. Therefore, (3) can be rewritten as

$$\tilde{k} = \frac{1 - \phi^{SF} + \frac{\left(\frac{W}{R_0}\right)}{\left(\frac{E_b}{N_t}\right)_{\text{REQ}}}}{N\left[1 - \phi^{SC} + \frac{(\phi^{SC}-\phi^{SF})}{N} + 10^{\frac{Z}{10}}\right]} \tag{54}$$

where the minimum data rate R_0 is assumed to be so low that the outage event does not occur.

Let us assume that total N_T users are waiting for the service in a BS. As shown in Fig. 2, transmission duration T can be given by $T = T_R/(N_T/N)$. We also assume one round robin period T_R to be so short that the propagation loss of each MS

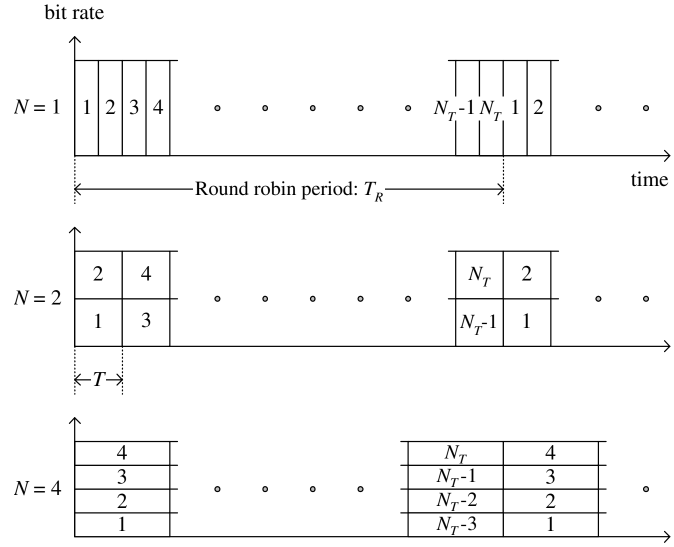

Fig. 2. Example of packet transmission with various numbers of simultaneous users.

is not changed during T_R. Let E_{T_R} be the effective transmitting data of BS during T_R. Then, it can be computed as the sum of data transmitted to each user. Therefore

$$\begin{aligned} E_{T_R} &\equiv (1-\text{BLER}) \sum_{j=1}^{N_T} T \cdot \tilde{k}_j \cdot R_0 \\ &= (1-\text{BLER}) \frac{R_0 T_R}{N_T} \\ &\quad \cdot \sum_{j=1}^{N_T} \frac{1 - \phi^{SF} + \frac{\left(\frac{W}{R_0}\right)}{\left(\frac{E_b}{N_t}\right)_{\text{REQ}}}}{1 - \phi^{SC} + \frac{(\phi^{SC}-\phi^{SF})}{N} + 10^{\frac{Z_j}{10}}} \end{aligned} \tag{55}$$

where the subscript j denotes the jth user.

We now discuss the relation between E_{T_R} and N with the following two conditions.

1) With the condition $\phi^{SC} < \phi^{SF}$, $(\phi^{SC} - \phi^{SF})/N$ in the previous equation becomes a negative number. Then, E_{T_R} is decreased with N. This result coincides with that shown in [5], where the multi-user interference alone was considered, i.e., $\phi^{SC} < 1$ and $\phi^{SF} = 1$.
2) With the condition $\phi^{SC} = \phi^{SF}$, $(\phi^{SC} - \phi^{SF})/N$ becomes zero. Then, E_{T_R} does not depend on N.

Considering the link level results in [3], it is believed that the latter condition is more realistic than the former. We can, therefore, say that the system throughput at full loading is the same, regardless of the number of users receiving data from a BS simultaneously.

$$p_C(C) = \begin{cases} \frac{1}{N\cdot n_{\max}} \sum_{m=0}^{N\cdot n_{\max}-1} d_m e^{-\frac{j2\pi\left(\frac{C}{R_0}\right)m}{N\cdot n_{\max}}}, & \text{for } R_0 \le C < C_{\max} \\ \sum_{n=\frac{C_{\max}}{R_0}}^{N\cdot n_{\max}} \left[\frac{1}{N\cdot n_{\max}} \sum_{m=0}^{N\cdot n_{\max}-1} d_m e^{-\frac{j2\pi nm}{N\cdot n_{\max}}}\right], & \text{for } C = C_{\max} \end{cases} \tag{51}$$

The simple comparison in this subsection confirms that the asymptotic throughput with CDS can be equal to that with TDS if the data rate set is continuous and unlimited.

B. 3GPP WCDMA System Model

The developed analysis in the previous section is applied to a system model based on a 3GPP WCDMA FDD release 1999 (R99) system. Downlink shared channel (DSCH) in [20] is selected as the packet channel model. The system parameters and the default values set for the analysis are listed in Table I.

The downlink orthogonal VSF (OVSF) codes are divided into three groups, as shown in Fig. 3. A branch of $\mathrm{SF} = 8$ in an OVSF code tree is assigned to the overhead channels. We analyze the case that 40% of the current BS power is allocated to the circuit channels, i.e., $\delta = 0.4$. Considering the speech services, we reserve three branches of $\mathrm{SF} = 8$ for the circuit channels. Hence, two branches of $\mathrm{SF} = 4$ are available for the packet channels. Considering modulation order and FEC code rate, $C_{\max}$ then becomes 1280 kb/s.

The cellular system is modeled by locating BSs at the centers of a hexagonal grid pattern, as shown in Fig. 4. An omnidirectional antenna pattern is used. To simplify the analytical procedure, the region A_0 is restricted to the sector of radius D_A and of angle $\pi/6$, as shown in the figure. Note that by symmetry, the relative position of users and BSs is the same throughout as for the sector of the figure. In the analytical model, we consider 11 BSs near BS_i. These BSs are influential in the received other cell interference of users located on A_0 and connected to BS_i. In Fig. 4, the distance from each adjacent BS to MS_j can be represented as a function of the MS_j's position (r, θ)

$$r_{1,j}(r,\theta) = \sqrt{D_{BS}^2 + r^2 - 2rD_{BS}\cos\left(\frac{\pi}{6} - \theta\right)} \quad (56)$$

$$r_{2,j}(r,\theta) = \sqrt{D_{BS}^2 + r^2 - 2rD_{BS}\cos\left(\frac{\pi}{6} + \theta\right)} \quad (57)$$

$$r_{3,j}(r,\theta) = \sqrt{D_{BS}^2 + r^2 - 2rD_{BS}\cos\left(\frac{\pi}{2} + \theta\right)} \quad (58)$$

$$r_{4,j}(r,\theta) = \sqrt{D_{BS}^2 + r^2 - 2rD_{BS}\cos\left(\frac{2\pi}{3} + \theta\right)} \quad (59)$$

$$r_{5,j}(r,\theta) = \sqrt{D_{BS}^2 + r^2 - 2rD_{BS}\cos\left(\frac{2\pi}{3} - \theta\right)} \quad (60)$$

$$r_{6,j}(r,\theta) = \sqrt{D_{BS}^2 + r^2 - 2rD_{BS}\cos\left(\frac{\pi}{2} - \theta\right)} \quad (61)$$

$$r_{7,j}(r,\theta) = \sqrt{D_{BS}^2 + r^2 - 2rD_{BS}\cos\left(\frac{\pi}{3} - \theta\right)} \quad (62)$$

$$r_{8,j}(r,\theta) = \sqrt{4D_{BS}^2 + r^2 - 4rD_{BS}\cos\left(\frac{\pi}{6} - \theta\right)} \quad (63)$$

$$r_{9,j}(r,\theta) = \sqrt{9D_{Cell}^2 + r^2 - 6rD_{Cell}\cos\theta} \quad (64)$$

$$r_{10,j}(r,\theta) = \sqrt{4D_{BS}^2 + r^2 - 4rD_{BS}\cos\left(\frac{\pi}{6} + \theta\right)} \quad (65)$$

$$r_{11,j}(r,\theta) = \sqrt{9D_{Cell}^2 + r^2 - 6rD_{Cell}\cos\left(\frac{\pi}{3} + \theta\right)}. \quad (66)$$

TABLE I
SYSTEM PARAMETERS AND DEFAULT VALUES

Parameters	Values
Chip rate (Mcps)	3.84
Modulation	QPSK
FEC rate	1/3
SF set	{256, 128, 64, 32, 16, 8, 4}
Data rate set (kbps)	{10, 20, 40, 80, 160, 320, 640}
$(E_b/N_t)_{REQ}$ at R_0 (10 kbps)	3.0 (dB) for BLER = 0.1
$C_{\max}$ (Mbps)	1.28
Path loss exponent, μ	4
Shadowing standard deviation, σ	10
Site-to-site correlation, b^2	0.5
Downlink orthogonality, ϕ	0, 0.25, 0.5, 0.75
Overhead channel power ratio, α	0.2
Circuit channel power ratio, δ	0.4

We apply the uniform distribution to the user location. Therefore

$$f(r,\theta) = \begin{cases} \frac{12r}{\pi D_A^2}, & \text{for } 0 < r \le D_A \text{ and } 0 \le \theta < \frac{\pi}{6} \\ 0, & \text{elsewhere} \end{cases}. \quad (67)$$

Let us summarize the analytical procedure. With the given values in Table I and the user distribution, we first compute the power usage efficiency $\bar{\beta}$ by using the numerical integrations and the iteration method, as shown in Section III-B. Next, we derive the PMF of the assigned data rate $p_R(R)$ by using the computed $\bar{\beta}$, as shown in Section III-A. Finally, we obtain the asymptotic throughput by using the derived $p_R(R)$, as shown in Section III-C.

We have also developed a computer simulation to validate the analytical results. The *Monte Carlo* simulation model consists of 19 cells of two tiers, and we collect data from the center cell for statistics.

C. Comparison in the System With the Limited Data Rate Set

In this subsection, numerical results in the system with the limited data rate set are presented. We compare the results from the various settings of the number of simultaneous users N.

Fig. 5 shows the PMFs of the data rate assigned to a user $p_R(R)$ for various settings of N. As N is increased, the maximum allowable power per user P^U is decreased, and then the data rate distribution moves toward the lower data rate. The figure also shows that $p_R(640\text{ kb/s})$ for $N = 1$ is abruptly higher than the others. It is because the highest assigned data rate is limited by the maximum allowable data rate, i.e., 640 kb/s, rather than interference power. We can also see that $p_R(20\text{ kb/s})$ and $p_R(10\text{ kb/s})$ for $N = 64$ are higher than other probabilities for $N = 2, \cdots, 32$. When $N = 64$, outage events occur due to too small P^U. Transmission opportunity for the outage user is reassigned to another user whose received E_b/N_t is above $(E_b/N_t)_{\mathrm{REQ}}$. Hence, the occurrence of 20 or 10 kb/s for $N = 64$ is more frequent than the others.

The results in Fig. 6 clarify that the assigned data rate can be determined by the peak data rate limitation. The figure shows the probability that the assigned data rate is limited by the given

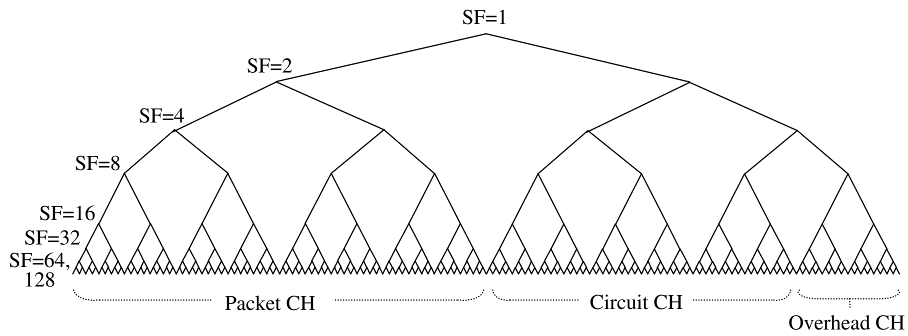

Fig. 3. OVSF code division.

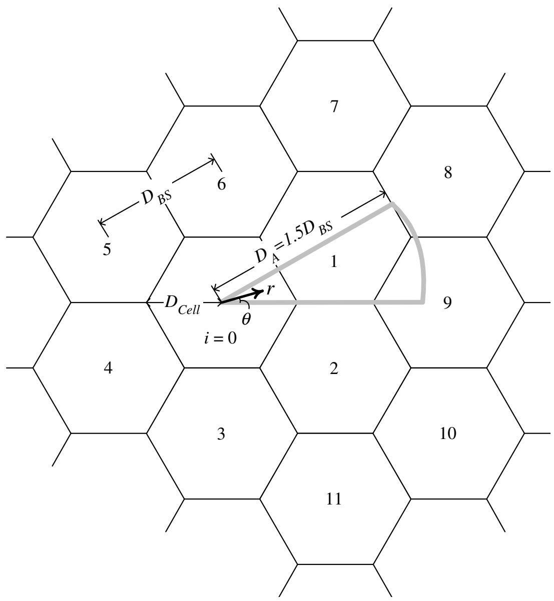

Fig. 4. Cell site deployment model.

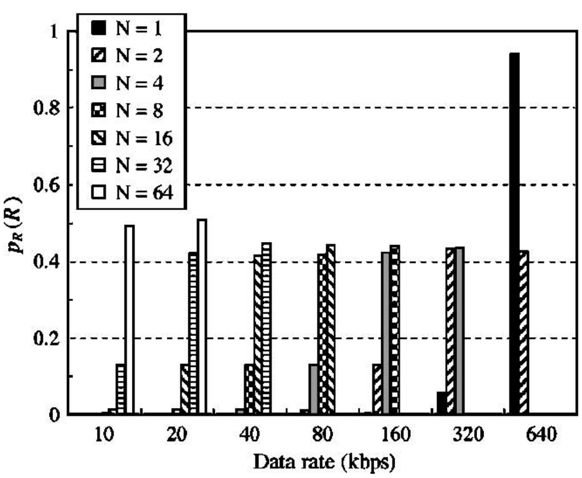

Fig. 5. PMF of the assigned data rate: $\phi = 0.5$.

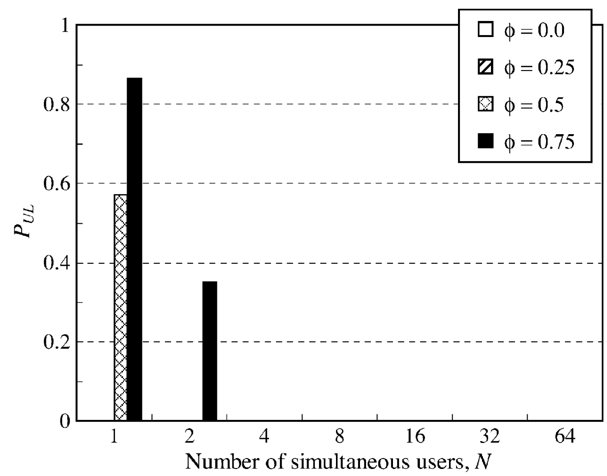

Fig. 6. Probability of the assigned data rate being limited by the data rate set.

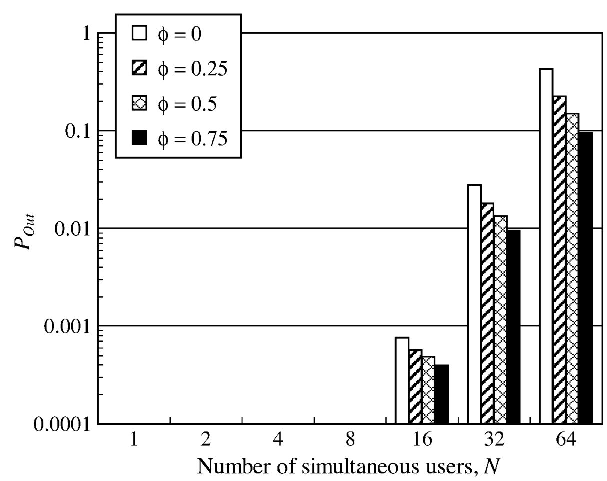

Fig. 7. Outage probability.

data rate set, i.e., P_{UL}, with various orthogonality factors. As mentioned previously, when $N = 1$ at $\phi = 0.5$, the highest assigned data rate is limited by the given data rate set. The figure shows that P_{UL} for $N = 1$ exceeds 50% at $\phi = 0.5$, and it is increased with ϕ. But, we can see that this effect of the limited data rate set can be avoided by increasing N.

Fig. 7 shows P_{Out} for various settings of N and ϕ. The outage probability P_{Out} is increased with N, contrary to P_{UL}. As N and ϕ are decreased, P_{Out} is increased because of too small P^U and high interference.

As ϕ gets higher, the total system throughput can be limited by the number of reserved OVSF codes rather than interference power. Fig. 8 shows that the code shortage occurs when ϕ is equal to or over 0.75 and N becomes 4. When $N \leq 2$, the system throughput is not affected by $C_{\max}$. It is because the

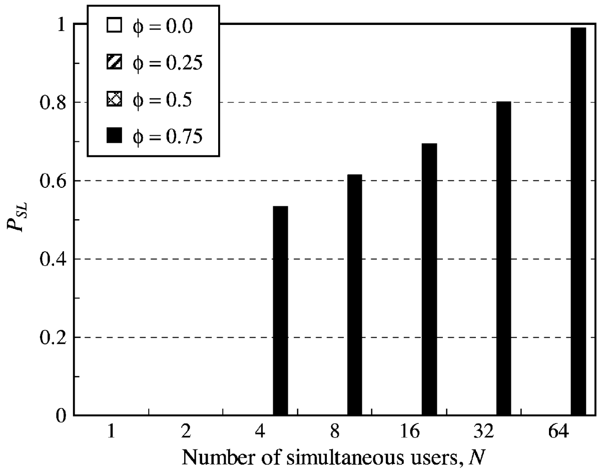

Fig. 8. Probability of the system throughput being limited by the number of reserved OVSF codes.

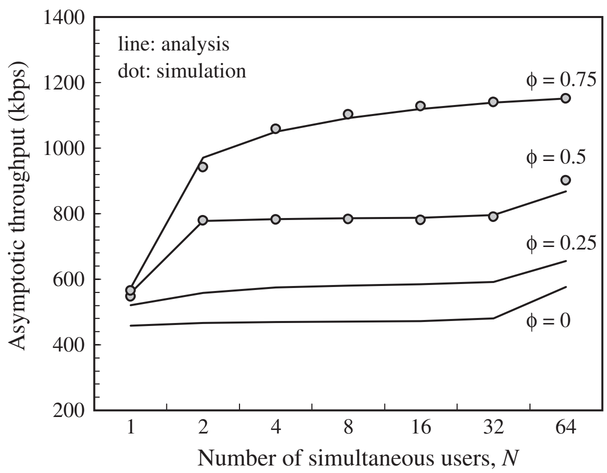

Fig. 9. System throughput.

assigned data rate to each user has already been limited by the given data rate set, i.e., $N \cdot R_{\max}(= N \cdot 640\ \text{kb/s}) \leq C_{\max}(= 1280\ \text{kb/s})$ for $N = 1$ and 2.

The asymptotic throughput is plotted as a function of N in Fig. 9. We can see that the asymptotic throughput is increased with N for all values of ϕ. When N is set to be low, the increase in the asymptotic throughput is due to the peak rate limitation of the data rate set. On the other hand, the increase for the high values of N is caused by the resource reallocation of users in the outage. For $2 \leq N \leq 32$ at $\phi \leq 0.5$, since P_{UL} and P_{Out} are zero and very low, respectively, the asymptotic throughput remains almost constant. The results in the figure show that CDS can outperform TDS with regard to the system throughput.

The simulation results for $\phi = 0.5$ and 0.75 are also shown in Fig. 9. In the analytical modeling, we applied two assumptions. One is that random variable β is assumed as a constant value $\bar{\beta}$ for simplicity. For checking this simplification, the randomness of β, depending on the shadowing component as well as user location, was simulated in our simulation program. Although this simplification has been employed in the analytical model, we can see that the analytical results for $\phi = 0.5$ agree with the simulation results.

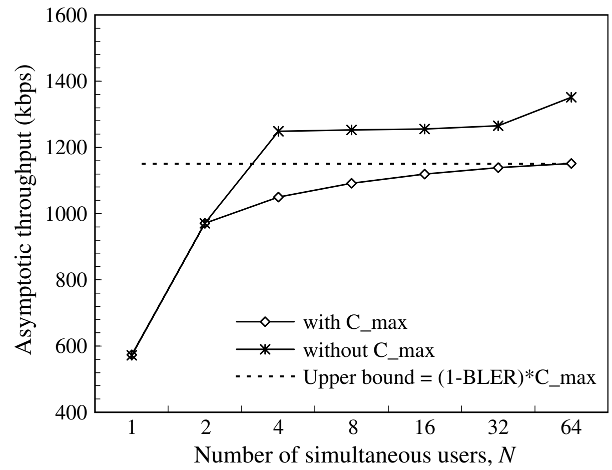

Fig. 10. Effect of code shortage on the system throughput: $\phi = 0.75$.

The other is that the data rates of N simultaneous users are assumed to be independent with another. This assumption is valid when a code shortage does not occur, such as $\phi \leq 0.5$. However, if the total data rate C is limited by the number of reserved OVSF codes, every user data rate can affect one another. For checking this assumption, we compare the analytical and the simulation results for the case when the code shortage occurs, i.e., $\phi = 0.75$. In Fig. 9, we can see that the two results match well even for $\phi = 0.75$.

In the last figure, we present the effect of code shortage on the system throughput. Fig. 10 shows the asymptotic throughputs for $\phi = 0.75$ with and without the limitation of OVSF codes $C_{\max}$. We can see that the reduction in the asymptotic throughput by $C_{\max}$ is too large to be neglected. This result confirms that the limitation of available spreading codes should be taken into consideration for the exact analysis.

Lastly, we discuss the impact of OVSF code division. Fig. 10 shows that both throughputs with and without $C_{\max}$ increase with N. This implies that, even if the OVSF code division is changed, CDS can still outperform TDS. As more branches in the OVSF code tree are allocated to the packet service, $C_{\max}$ increases. Then, a code shortage problem may be avoided and the throughput can be increased. However, as shown in Fig. 10, the throughput with CDS is still equal to or higher than that with TDS. We believe that the claim of this paper would not be affected with other values of OVSF code division applied.

V. Conclusion

The system throughputs with CDS and TDS have been compared on the multirate CDMA downlink. Analytical models and methodologies have been developed for the performance evaluation.

We have shown that if the data rate set is continuous and unlimited, the system throughput at full loading can be the same with both multiplexing schemes applied. This implies that the asymptotic throughput may be the same, regardless of the number of users receiving data from a BS simultaneously. The link level analysis [3] has already shown that the link performance degradation caused by the self-interference is approximately equal to that by the multi-user interference.

However, the self-interference has been neglected in many system level analyses [5], [21]. Our results confirm that the effect of self-interference can be the same as that of multi-user interference on the system performance.

We also presented the effect of the limited data rate set on the asymptotic throughput. When the number of simultaneous users is less, the asymptotic throughput is low because the peak data rate for a user is limited in practical systems. On the other hand, as the number of simultaneous users is increased, the throughput gets higher. This is because more resources can be allocated to the users in good channel conditions. Therefore, the outage probability can get higher with this improvement in throughput. It is also shown that the asymptotic throughput can be limited when the available number of spreading codes is not enough. It may happen when the orthogonality is well preserved in the radio link. From the overall results, it is shown that CDS may outperform TDS with respect to the asymptotic system throughput when we take into account the self-interference, the limitation on the data rate set, and resource reallocation of users in outage.

The analytical results have been compared with that of the *Monte Carlo* simulation. The comparison shows that the analytical and simulation results are in very good agreement which confirms that we can use the analytical method proposed in this paper with confidence. We believe that the proposed models and analytical methods can be utilized for developing various control schemes for the downlink packet transmission and also for predicting the performance of CDMA downlink packet communication systems.

References

[1] H. Holma and A. Toskala, *WCDMA for UMTS*. New York: Wiley, 2000.

[2] E. Dahlman and K. Jamal, "Wide-band services in a DS-CDMA based FPLMTS system," in *Proc. IEEE 46th Vehicular Technology Conf. (VTC)*, Atlanta, GA, Apr. 1996, pp. 1656–1660.

[3] M. Latva-aho, "Bit error probability analysis for FRAMES WCDMA downlink receivers," *IEEE Trans. Veh. Technol.*, vol. 47, pp. 1119–1133, Nov. 1998.

[4] S. Ramakrishna and J. M. Holtzman, "A scheme for throughput maximization in a dual-class CDMA system," *IEEE J. Select. Areas Commun.*, vol. 16, pp. 830–844, June 1998.

[5] A. Bedekar, S. Borst, K. Ramanan, P. Whiting, and E. Yeh, "Downlink scheduling in CDMA data networks," in *Proc. IEEE Global Telecommunications Conf. (GLOBECOM)*, Rio de Janeiro, Brazil, Dec. 1999, pp. 2653–2657.

[6] M. Airy and K. Rohani, "QoS and fairness for CDMA packer data," in *Proc. IEEE 51st Vehicular Technology Conf. (VTC)*, Tokyo, Japan, May 2000, pp. 450–454.

[7] F. Adachi, M. Sawahashi, and K. Okawa, "Tree-structured generation of orthogonal spreading codes with different lengths for forward link of DS-CDMA mobile radio," *Electron. Lett.*, vol. 33, no. 1, pp. 27–28, Jan. 1997.

[8] H. Furukawa, "Theoretical capacity evaluation of power controlled CDMA downlink with code limitation," in *Proc. IEEE 51st Vehicular Technology Conf. (VTC)*, Tokyo, Japan, May 2000, pp. 997–1001.

[9] *Radio Resource Management Strategies (Release 1999)*, 3GPP 3G TR 25.922, V3.5.0, Mar. 2001.

[10] *Physical Layer Procedure (FDD) (Release 1999)*, 3GPP 3G TR 25.214, V3.7.0, June 2001.

[11] A. J. Viterbi, A. M. Viterbi, K. S. Gilhousen, and E. Zehavi, "Soft handoff extends CDMA cell coverage and interferences reverse link capacity," *IEEE J. Select. Areas Commun.*, vol. 12, pp. 1281–1288, Aug. 1994.

[12] M. Pratesi, F. Santucci, F. Graziosi, and M. Ruggieri, "Outage analysis mobile radio systems with generically correlated log-normal interferers," *IEEE Trans. Commun.*, vol. 48, pp. 381–385, Mar. 2000.

[13] P. R. Patel, U. S. Goni, E. Miller, and P. P. S. Carter, "A simple analysis of CDMA soft handoff gain and its effect on the cell's coverage area," in *Proc. 15th WINLAB Workshop*, East Brunswick, NJ, Apr. 1995, pp. 101–118.

[14] M. Zorzi, "On the analytical computation of the interference statistics with applications to the performance evaluation of mobile radio systems," *IEEE Trans. Commun.*, vol. 45, pp. 103–109, Jan. 1997.

[15] J. Cho and D. Hong, "Statistical model of downlink interference for the performance evaluation of CDMA systems," *IEEE Commun. Lett.*, vol. 6, pp. 494–496, Nov. 2002.

[16] A. Papoulis, *Probability, Random Variables, and Stochastic Processes*, 3rd ed. New York: McGraw-Hill, 1991.

[17] E. Kreyszig, *Advanced Engineering Mathematics*, 8th ed. New York: Wiley, 1999.

[18] A. Leon-Garcia, *Probability and Random Processes for Electrical Engineering*. Reading, MA: Addison-Wesley, 1994.

[19] M. Ahmed, M. Airy, and K. Rohani, "Spectral efficiency estimates for CDMA2000—A third generation cellular standard," in *Proc IEEE 49th Vehicular Technology Conf. (VTC)*, Houston, TX, May 1999, pp. 361–365.

[20] *Physical Channels and Mapping of Transport Channels Onto Physical Channels (FDD) (Release 1999)*, 3GPP 3G TS 25.211, V3.7.0, June 2001.

[21] C. Mihailescu, X. Lagrange, and P.Ph. Godlewski, "Radio resource management for packet transmission in UMTS WCDMA system," in *Proc. IEEE 50th Vehicular Technology Conf. (VTC)*, Amsterdam, The Netherlands, Sept. 1999, pp. 573–577.

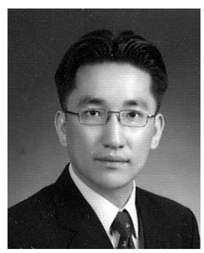

Jaeweon Cho (S'95–M'03) received the B.S. (*magna cum laude*), M.S., and Ph.D. degrees in electronic engineering from Sogang University, Seoul, Korea, in 1995, 1997, and 2002, respectively.

From 1997 to 1998, he was with the Research and Development Center, DACOM, Korea. Since 2002, he has been a Postdoctoral Associate in the School of Electrical and Computer Engineering, Cornell University, Ithaca, NY. His research interests include wireless communications and the next generation network issues, particularly the network architectures, control algorithms, and performance analysis.

Dr. Cho is a member of the Korean Institute of Communication Sciences (KICS).

Daehyoung Hong (S'76–M'86) received the B.S. degree in electronics engineering from the Seoul National University, Seoul, Korea, in 1977, and the M.S. and Ph.D. degrees in electrical engineering from the State University of New York, Stony Brook, in 1982 and 1986, respectively.

He was a Faculty Member of the Electrical and Electronics Engineering Department, ROK Air Force Academy and an Air Force Officer from 1977 to 1981. He joined Motorola Communication Systems Research Laboratory, Schaumburg, IL, in 1986, where he was a Senior Staff Research Engineer and participated in the research and development of digital trunked radio systems (TRS) as well as CDMA digital cellular systems. He joined the faculty of the Electronic Engineering Department, Sogang University, Seoul, Korea, in 1992, where he is currently a Professor. During the academic year 1998 to 1999 he was a Visiting Associate Professor at the University of California, San Diego, working there with the Center for Wireless Communications. His research interests include design, performance analysis, control algorithms, and operations of wireless access network and communication systems. He has published numerous technical papers and holds several patents in the areas of wireless communication systems. He has been a consultant for a number of industrial firms.

Dr. Hong is a member of the Korea Institute of Communication Sciences (KICS) and Institute of Electronic Engineers Korea (IEEK). He has been active in a number of professional societies. His service includes: Chairman, Korea Chapter, IEEE Communications Society; Chairman, Mobile Communications Technical Activity Group, KICS; Chairman, Communications Society, IEEK; and technical program committees for several major conferences. He served as a Division Editor for Wireless Communications of the *Journal of Communications and Networks*. He is now Vice Director of the Asia Pacific Region of the IEEE ComSoc.